Spatially Looped Algorithms for Time-Domain Analysis of Periodic Structures

Malgorzata Celuch-Marcysiak and Wojciech K. Gwarek, *Senior Member, IEEE*

***Abstract*—A class of spatially looped time-domain algorithms is developed. These algorithms prove to be effective tools for the analysis of microwave periodic structures. They use the FDTD or TLM simulation of only one spatial period, with a new type of boundary condition modeling its behavior in the entire structure. Applications to a sinusoidally corrugated slow wave structure and to a four-wall corrugated waveguide are presented. The paper includes a tutorial part, discussing the physical nature of solutions produced by the spatially looped algorithms. This explains the meaning of complex notation in the time domain, and the possibility of reducing the calculations of uniform and periodic guiding structures to real numbers.**

I. Introduction

During the last decade, time-domain electromagnetic simulation has become a popular tool among the microwave community. Its advantages include efficiency in providing circuit characteristics over a wide frequency band, as well as flexibility in studying arbitrary geometries, inhomogeneous and anisotropic media, and transient processes. However, a 3-D time-domain analysis requires extensive computer resources. Therefore, significant research effort is directed toward exploiting various kinds of spatial symmetry and regularity, in order to reduce the computing memory and time.

Let us recall that a more classical frequency-domain approach to the electromagnetic analysis originates from the well-known separation of space and time variables. By applying the Fourier transform in time, the original problem is projected into the frequency domain where (in the case of linear circuits) solutions are sought for each value of frequency separately, in terms of the three space variables.

Recently, an analog of this approach has been adapted for the time-domain analysis of structures uniform along one spatial dimension, such as transmission lines aligned with the z-axis. The z-variable can then be separated, and the Fourier transform projects the physical z-domain into the phase shift-domain (β_z-domain). Electromagnetic simulation is conducted as a function of two space variables and time, for each value of β_z separately. By eliminating one variable, savings in computer resources of over an order of magnitude result. Such an approach led to several algorithms reported in recent years, such as the ones using complex notation in TLM [1], [2] and FDTD [3], [4] or real notation in FDTD [5], [6] and TLM [7], [8].

Manuscript received October 11, 1993; revised August 8, 1994.

The authors are with the Institute of Radioelectronics, Warsaw University of Technology, 00-665 Warsaw, Poland.

IEEE Log Number 9408568.

Moreover, in [5] and [6], the above approach has also been applied to several classes of microwave problems other than uniform transmission lines, such as the full-wave analysis of axisymmetrical circuits (with Fourier transform applied in the ϕ-domain) or the characterization of E-plane waveguide discontinuities (with Fourier transform applied in the x-domain).

In this paper, we further elaborate on a method for analyzing microwave circuits periodic along one spatial dimension. We focus on periodic structures of propagation which play an important role in microwave research and engineering, for example, in ultrahigh power pulse generation [9] and in antenna systems [10], [11]. When compared to uniform guiding structures (UGS), the difficulty in analyzing periodic guiding structures (PGS) stems from the fact that solutions in PGS cannot be sought for each value of β_z separately. Any mode in a periodic structure with a fundamental phase constant β_{zo} comprises an infinite series of so-called space harmonics with phase constants $\pm\beta_{zo} \pm 2m\pi/L$, where L is the length of one period (Fig. 1) and $m = 1, 2, \cdots$.

In Section II of this paper, we show that a rigorous analysis of PGS (taking into account the space harmonics) can be conducted in the time domain, based on the FDTD or TLM modeling of only one period of the structure. We derive a special form of periodic boundary conditions which "loop" the model. Further in the paper, we shall consider the spatially looped FDTD algorithm as a reference, but explanatory remarks concerning the TLM formulation will also be given.

Traditionally, periodic structures have been treated in the frequency domain [9], [11]. The spatially looped algorithms of this paper maintain classical advantages of the time-domain approach, and consequently they can be considered as an interesting alternative in a range of applications to PGS. This will be demonstrated by means of examples in Section III. Here, let us only stress that the spatially looped time-domain algorithms can be applied to PGS of arbitrary shape and inhomogeneous filling, and that there are no problems with investigating higher passband modes in slow-wave structures.

In Section IV, we provide physical insight into the field distribution produced by the spatially looped algorithms. The objective is to explain combined use of the time-domain and phase shift-domain representation of electromagnetic fields. Since analogous representation has been previously used for UGS, our discussion reveals new (and somewhat surprising) interpretations of the recent FDTD and TLM algorithms of [1]–[8].

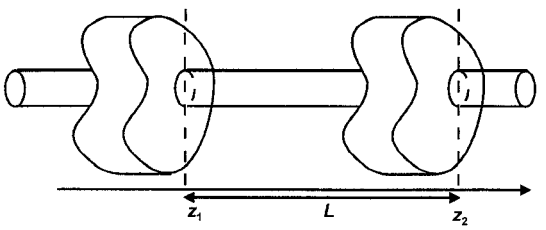

Fig. 1. General periodic structure with period L.

II. Derivation of Spatially Looped Algorithms

We refer to a general microwave structure, periodic with respect to the $z-$coordinate (Fig. 1). We discretize one period of this structure ($z_1 \leq z < z_2$) into basically cubicoid cells; but in the $xy-$plane, we also use modified cells [12] to improve the representation of curved geometries. Although we can vary cell lengths along the z-axis, for simplicity let us assume that $\Delta z = \text{const}$; we then require that $L = (z_2 - z_1) = N\,\Delta z$ where N is an integer.

Now we aim to define appropriate longitudinal boundary conditions, modeling periodicity of the structure. This will lead us to two versions of the spatially looped FDTD algorithm, expressed in the complex and real notation, respectively.

A. Looped FDTD—Complex Version (CL-FDTD)

Assume that the structure of Fig. 1 supports a wave of the fundamental propagation vector $\beta_{zo}\boldsymbol{i}z$. Then, according to the Floquet theorem [13], the z-dependence of any field component is given by function $f(z)$

$$f(z) = f'(z)e^{\pm j\beta}zo^{z} \tag{1}$$

where $f'(z)$ is periodic with period L.

In the FDTD algorithms, we analyze fields as a function of three space variables and time. In view of (1), for one traveling wave we can express the fields as follows:

$$\begin{aligned}\boldsymbol{E}(x, y, z, t) &= \boldsymbol{E}'(x, y, z, t)e^{-j(\beta_{zo}z+\varphi)}\\ \boldsymbol{H}(x, y, z, t) &= \boldsymbol{H}'(x, y, z, t)e^{-j(\beta_{zo}z+\varphi)}\end{aligned} \tag{2}$$

where functions $\boldsymbol{E}'_{\perp}(x, y, z, t)$ and $\boldsymbol{H}'_{\perp}(x, y, z, t)$ are real, functions $\boldsymbol{E}'_{z}(x, y, z, t)$ and $\boldsymbol{H}'_{z}(x, y, z, t)$ are imaginary, and all functions $\boldsymbol{E}'(x, y, z, t)$ and $\boldsymbol{H}'(x, y, z, t)$ are periodic with respect to the z-variable, with period L (Fig. 1), so that, in particular,

$$\boldsymbol{E}'(x, y, z_2, t) = \boldsymbol{E}'(x, y, z_1, t)$$

$$\boldsymbol{H}'(x, y, z_2 - \Delta z/2, t) = \boldsymbol{H}'(x, y, z_1 - \Delta z/2, t). \tag{3}$$

Note that in (2), the time-domain representation of electromagnetic fields is maintained. Complex notation results from applying the Fourier transform only in space, in the z-domain.

To take advantage of properties (2) and (3) in the FDTD analysis of PGS, we must represent each field by a real and imaginary component:

$$\begin{aligned}\boldsymbol{E}(x, y, z, t) &= \boldsymbol{E}'(x, y, z, t)\cos(\beta_{zo}z + \varphi)\\ &\quad - j\boldsymbol{E}'(x, y, z, t)\sin(\beta_{zo}z + \varphi)\end{aligned}$$

$$\begin{aligned}\boldsymbol{H}(x, y, z, t) &= \boldsymbol{H}'(x, y, z, t)\cos(\beta_{zo}z + \varphi)\\ &\quad - j\boldsymbol{H}'(x, y, z, t)\sin(\beta_{zo}z + \varphi).\end{aligned} \tag{4}$$

Let us first assume that the medium filling the structure is lossless and described by real functions $\epsilon(x, y, z)$, $\mu(x, y, z)$ (extension to other media will be considered in Section IV). The discretized Maxwell operators are real and linear, and inside the model ($z_1 \leq z \leq z_2 - \Delta z/2$) the real and imaginary components of (4) are decoupled. Thus, inside the model, we conduct the FDTD simulation on the real and imaginary grids independently, using standard 3-D FDTD equations. We couple the two grids in planes separated by one period of the structure, imposing the following boundary conditions for the tangential E- and H-fields:

$$\boldsymbol{E}_{\perp}(x, y, z_2, t) = \boldsymbol{E}_{\perp}(x, y, z_1, t)e^{j\psi}$$

$$\begin{aligned}&\boldsymbol{H}_{\perp}(x, y, z_1 - \Delta z/2, t + \Delta t/2)\\ &\quad = \boldsymbol{H}_{\perp}(x, y, z_2 - \Delta z/2, t + \Delta t/2)e^{-j\psi}\end{aligned} \tag{5}$$

where $\psi = (z_2 - z_1)\,\beta_{zo} = \beta_{zo}L$ is the assumed fundamental phase shift per period. entering the program as a parameter.

In the TLM formulation of our method, all incident and reflected pulses ${}^{i}V$, ${}^{r}V$ are represented by real and imaginary components

$$\begin{aligned}{}^{\mathrm{i}}V(x, y, z, t) &= {}^{\mathrm{i}}V'(x, y, z, t)\cos(\beta_{zo}z + \varphi)\\ &\quad - j\,{}^{\mathrm{i}}V'(x, y, z, t)\sin(\beta_{zo}z + \varphi)\\ {}^{\mathrm{r}}V(x, y, z, t) &= {}^{\mathrm{r}}V'(x, y, z, t)\cos(\beta_{zo}z + \varphi)\\ &\quad - j\,{}^{\mathrm{r}}V'(x, y, z, t)\sin(\beta_{zo}z + \varphi)\end{aligned} \tag{6}$$

where functions ${}^{r}V'$, ${}^{i}V'$ are real and periodic with period L. Within the model, scattering is performed on the real and imaginary grids separately. The two grids are coupled by the periodic boundary conditions

$$\begin{aligned}{}^{\mathrm{i}}V(x, y, z_2, t) &= {}^{\mathrm{r}}V(x, y, z_1, t)e^{-j\psi}\\ {}^{\mathrm{i}}V(x, y, z_1, t) &= {}^{\mathrm{r}}V(x, y, z_2, t)e^{j\psi}.\end{aligned} \tag{7}$$

We first simulate wave propagation in the system with the assumed phase shift ψ, using pulse excitation. Fourier analysis of the circuit's response indicates all frequencies for which the propagation is possible (that is, all the modes which can propagate and give the assumed fundamental phase shift per period). Subsequently, we can excite the circuit by a sinusoidal signal of a particular frequency (applying the excitation scheme of [7]), and when the steady state is reached, we obtain field distribution for a particular mode.

In the case of uniform guiding structures E' and H' in (2) and (4) do not depend on z, thus an arbitrary length of the period L can be assumed. When choosing $L = \Delta z\,(N = 1)$, we obtain the complex algorithms applied by Jin *et al.* in the SCN TLM notation [1] and in FDTD [4], and by Arndt *et al.* in FDTD [3].

B. Looped FDTD—Real Version (RL-FDTD)

Let us consider a standing wave in the structure of Fig. 1. From (2), the expressions for fields are as follows:

$$\begin{aligned}
&\boldsymbol{E}_\perp(x, y, z, t) = \boldsymbol{E}'_\perp(x, y, z, t)\cos(\beta_{zo}z + \varphi)\\
&\boldsymbol{H}_\perp(x, y, z, t) = \boldsymbol{H}'_\perp(x, y, z, t)\sin(\beta_{zo}z + \varphi)\\
&\quad \cdot E_z(x, y, z, t) = E'_z(x, y, z, t)\sin(\beta_{zo}z + \varphi)\\
&\quad \cdot H_z(x, y, z, t) = H'_z(x, y, z, t)\cos(\beta_{zo}z + \varphi). \quad (8)
\end{aligned}$$

Periodic boundary conditions are modeled by spatial looping of fields

$$\boldsymbol{E}_\perp(x, y, z_2, t) = T_E(\psi, \varphi)\boldsymbol{E}_\perp(x, y, z_1, t)$$

$$\begin{aligned}
&\boldsymbol{H}_\perp(x, y, z_1 - \Delta z/2, t + \Delta t/2)\\
&\quad = T_H(\psi, \varphi)\boldsymbol{H}_\perp(x, y, z_2 - \Delta z/2, t + \Delta t/2) \quad (9)
\end{aligned}$$

with looping operators $T_E(\psi, \varphi)$, $T_H(\psi, \varphi)$ given by

$$\begin{aligned}
T_E(\psi, \varphi) &= \frac{\cos(\psi + \varphi)}{\cos(\varphi)}\\
T_H(\psi, \varphi) &= \frac{\sin(\varphi - 0.5\psi/N)}{\sin(\varphi + \psi - 0.5\psi/N)}. \quad (10)
\end{aligned}$$

In the above relations, ψ and N have the meaning as defined for the complex version of the algorithm. Angle φ allocates the analyzed period of the structure with respect to the standing wave waveform (see Fig. 6). Since calculations are limited to the real grid, the RL-FDTD algorithms saves half of the computer resources required by CL-FDTD, but it is numerically less robust. Physically, this is associated with numerical energy fluctuations in the model which we demonstrate in Section IV. Mathematically, calculations become unstable for values of ψ and φ such that $|T_E| > 1$ or $|T_H| > 1$.

Let us emphasize that there are no stability problems in our previous real algorithms for the analysis of UGS in the FDTD [5], [6] and SCN TLM [7], [8] versions. In fact, for single-layer models of UGS, the RL-FDTD of this paper *does not* reduce to the real FDTD algorithm of [5]. A basic difference is that in [5]–[8] only the $\boldsymbol{E}_\perp$ and H_z are considered on the real grid, while the $\boldsymbol{H}_\perp$ and E_z fields are on the imaginary grid. This ensures that all field components are considered at their maxima with respect to the z-coordinate, and numerical energy in the model remains constant in time.

III. Examples of Application

Our first example (Fig. 2) relates to a sinusoidally corrugated slow wave structure recently studied by Guo *et al.* [9]. Taking advantage of the axial symmetry of the problem, we use 2-D modeling in terms of the E_ρ, E_z, and H_ϕ field components, as explained in [5] and [6]. Periodic boundary conditions (5) are imposed for E_ρ and H_ϕ. We set a basic cell size to $\Delta x = \Delta y = 0.835$ mm. Thus, the model consists of 350 cells, including modified cells [12] which match the sinusoidal boundary. Computer storage requirements for the complex and real versions of the looped 2-D FDTD are 6 and 3 real variables per cell, respectively. The computing time on a PC 486 per one value of β_{zo} (producing resonances in all considered passbands simultaneously) is about 30 s for CL-FDTD and 15 s for RL-FDTD. Typically, results of CL-FDTD and RL-FDTD are indistinguishable. We find it advisable to establish cutoff frequencies by CL-FDTD and to use RL-FDTD for detailed plotting of the characteristics.

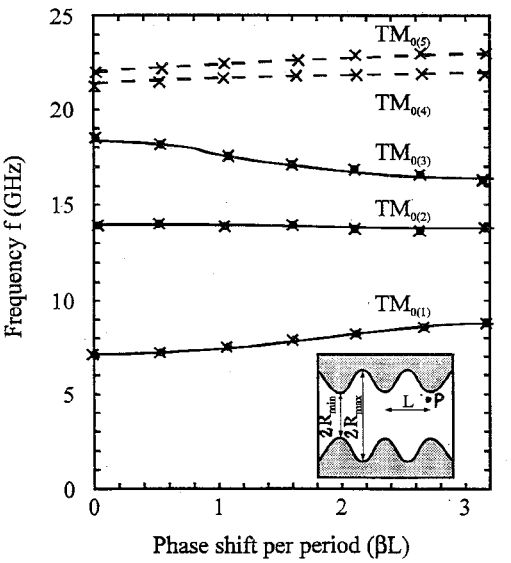

Fig. 2. Slow wave structure after [9] and its dispersion characteristics: •: measurements [9], ——: calculations [9], –×–: present algorithms; $R_{\min} = 1.397$ cm, $R_{\max} = 1.943$ cm, $L = 1.67$ cm.

As shown in Fig. 2, for the first three passbands of the axisymmetric TM mode, we obtain results in perfect agreement with the numerical and experimental data of [9]. For higher passbands, no reference has been given in [9], and difficulties in distinguishing the characteristics have been reported. Our method immediately provides these characteristics. Note that the $TM_{0(4)}$ and $TM_{0(5)}$ curves are close to each other, and almost perpendicular to the frequency axis. This explains why they are difficult to distinguish, when classically plotted as a function of frequency [9]. In our modeling results are sought versus phase shift. Thus, the structure resonates at one specific frequency in each passband, and a point on the dispersion characteristics is determined without ambiguity. Moreover, the field distribution can be monitored for any values of phase shift and frequency which facilitates correct naming of the modes.

Our second example concerns a four-wall corrugated waveguide (Fig. 3). We consider "odd-odd" modes generated by TE_{mn} and TM_{mn} of the smooth-walled guide with m, n odd. Thus, we can model one quadrant of one period. We set $\Delta z = 0.25$ mm, $\Delta x = \Delta y = 0.5$ mm, which gives 2640 cells. In 3-D modeling, each cell is described by 12 and 6 real variables in CL-FDTD and RL-FDTD, respectively. The computing time per one value of β_{zo} is about 15 min. for CL-FDTD and 8 min. for RL-FDTD.

Results of our method are in good agreement with the mode-matching after [11], as we show in Fig. 6. In [14], we have reported the agreement for the "odd-even" modes. A basic advantage of our method over mode-matching resides in its flexibility: structures with arbitrary (also continuous) variation of shape in the z-direction and with inhomogeneous

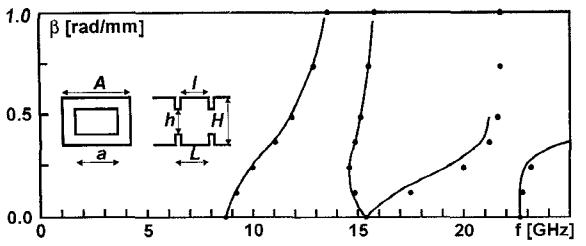

Fig. 3. Four-wall corrugated waveguide after [11] and dispersion characteristics for the "odd-odd" modes. ——: results of [11], •: present algorithms; $A = 33.02$ mm, $a = 22.86$ mm, $H = 20.32$ mm, $H = 10.16$ mm, $L = 1.01$ mm, $l = 1$ mm.

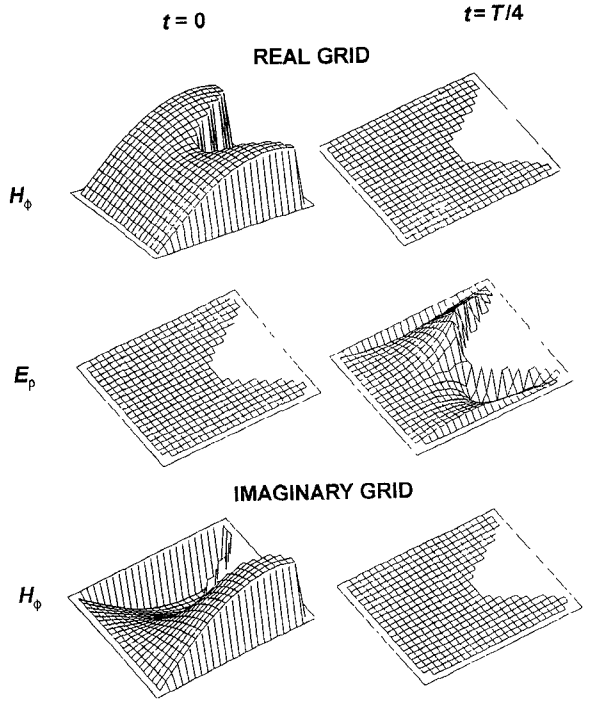

Fig. 4. Field distribution excited through real H_ϕ at point P in Fig. 2; $f = 7.717$ GHz, $\psi = \Pi/3$.

and anisotropic filling are analyzed without any modification of the computer code.

IV. Physical Interpretations

In this section, we explain the consequences of the combined time-domain/phase shift-domain representation of electromagnetic fields. Such a representation is inherent in the spatially looped algorithms of this paper and in previous algorithms [1]–[8] for the analysis of UGS. We shall refer to the sinusoidally corrugated structure of Fig. 2. We consider field distribution for the dominant $TM_{0(1)}$ mode at $f = 7.717$ GHz, $\psi = \Pi/3$ over one-half of the long-section of one period.

A. Eigensolutions of Complex Looped Algorithms

We apply sinusoidal excitation to a single field component—real H_ϕ at point P in Fig. 2. The distributions of E_ρ and H_ϕ on the real grid are presented in Fig. 4. It is clearly a standing wave pattern. This may seem surprising since we have forced a phase shift $\psi > 0$ corresponding to the propagation vector $\beta_{zo} i_z$ directed from left to right. Insight into the method brings the explanation: when the complex notation is applied to close the spatial loop, the sinusoidal waveforms due to the $\sin(\omega t)$ source decompose into ω and $-\omega$ spectral components. We obtain two traveling waves of phase velocities $v = \omega/\beta_{zo}$ and $v = -\omega/\beta_{zo}$, and of equal amplitudes. Their superposition produces a standing wave.

In the condensed node TLM formulation of the method, a basic way to apply the excitation is by a train of real pulses incident from an elementary transmission line at P. This evokes two standing waves since a pulse couples to both E- and H-field at P. Either one or both these fields are transversal. Therefore, superposition of the two waves is:

- a purely standing wave if the excitation line is perpendicular to the z-axis,
- a partially standing wave if the excitation line is parallel to the z-axis.

Intuitively, the notion of "a traveling wave resonator" has been proposed by Jin *et al.* [1] for a single-layer model of UGS described in the complex TLM notation. In view of the above discussion, we propose to use the name of "a periodic boundary resonator" as more appropriate.

B. Extension of Looped Algorithms to Media Described by Complex Parameters

Many practical media are described by complex parameters in the frequency domain, for example, $\mu = \mu' + j\mu''$. At first sight, it seems that complex parameters can be incorporated into the complex looped algorithms by coupling of the real and imaginary grids within the model. We shall briefly explain why this approach is physically incorrect.

Referring to the time-domain representation of fields, μ'' plays the role of a proportionality coefficient between the time-sinusoidal component of the H-field and time-cosinusoidal component of the B-field (or vice-versa) at the same point in space. Yet in Fig. 4 we observe that the H_ϕ waveforms emulated by CL-FDTD on the real and imaginary grids are in phase in time. Moreover, they correspond to two different locations in space, shifted by one-quarter of the fundamental wavelength, as predicted by (4). The spatial orthogonality of the two grids in the complex time-domain algorithms is best seen for UGS where (4) simplifies to

$$\boldsymbol{H}(x, y, z, t) = \boldsymbol{H}'(x, y, t)[\cos(\beta_z z + \varphi) - j \sin(\beta_z z + \varphi)]. \quad (11)$$

Complex media parameters and losses can be considered in the spatially looped time-domain algorithms only indirectly, in a way previously established for UGS [1], [2], [8]. In [8], we have shown that the indirect approach applies to the algorithms expressed in the real as well as complex notation.

C. Emulation of a Traveling Wave in Complex Looped Algorithms

We apply sinusoidal excitation to the real component of the H_ϕ field at P and cosinusoidal excitation to the imaginary

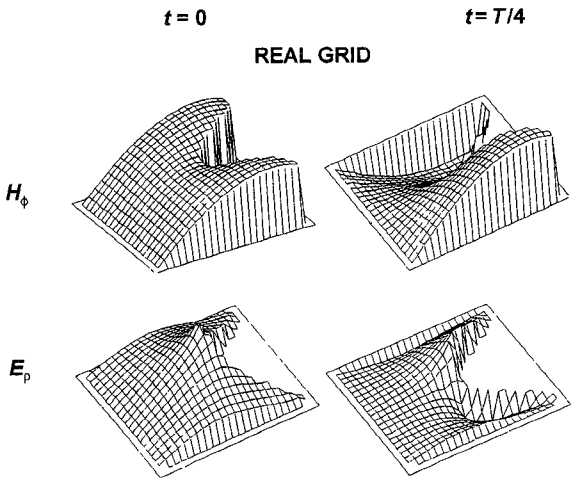

Fig. 5 . Field distribution invoked through sinusoidal excitation of real H_ϕ and cosinusoidal excitation of imaginary H_ϕ at P in Fig. 2; $f = 7.717$ GHz, $\psi = \Pi/3$.

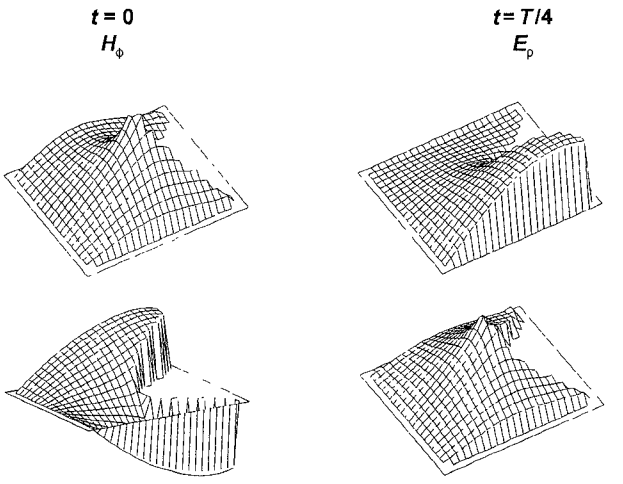

Fig. 6. Field distribution in the structure of Fig. 2 at $f = 7.717$ GHz, $\psi = \Pi/3$ as produced by RL-FDTD for (a) $\varphi = 0$ and (b) $\varphi = 0.9 \times \Pi/3$.

component of H_ϕ also at P. We shall call this "double orthogonal excitation" since it evokes two standing waves orthogonal in time and [in view of the preceding remarks, i.e., equations (4) and (11)] also in space. Their superposition is a traveling wave, as shown in Fig. 5.

In the complex looped TLM algorithms, we can also emulate a traveling wave by means of double orthogonal excitation, that is, by simultaneously applying a sinusoidally modulated train of real pulses and a cosinusoidally modulated train of imaginary pulses to the same node, through the same line.

Double orthogonal excitation requires longer computing time to converge to the steady state than the excitation by a single sinusoidal source. For tutorial purposes, it provides visualization of field intensities in PGS in the traveling wave regime, and it simplifies the study of power flow.

D. Properties of the RL-FDTD Algorithm

In RL-FDTD, the analysis is reduced to one standing wave, with nodes unambiguously located by parameter φ of (8), as shown in Fig. 6. In case of Fig. 6(b), the H_ϕ node coincides with point P, and the H_ϕ excitation at P becomes ineffective. To evoke the wave of Fig. 6(b), the source had to be shifted by a few cells. Such constraints do not exist in CL-FDTD, where the maximum of the standing wave automatically adjusts to the position of the source.

The RL-FDTD model is susceptible to large energy fluctuations. At $t = 0$, total energy of the model of Fig. 6(b) is contained in a section of the H_ϕ standing wave near its node; then it increases, and at $t = T/4$ it corresponds to E_ρ near its maximum (plus minor energy due to E_z). In CL-FDTD, energy remains constant in time since it can circulate between the two space-orthogonal grids.

V. Conclusion

We have introduced a class of spatially looped algorithms in the time domain. These algorithms are effective and accurate tools for the analysis of microwave periodic structures of arbitrary shape and inhomogeneous filling. They use the FDTD of TLM simulation of only one period of the structure, closing the loop between the longitudinal boundaries by means of periodic boundary conditions derived from the Floquet theorem. Dispersion characteristics are plotted as a function of phase shift per period. This ensures noteworthy precision for slow wave characteristics which are almost perpendicular to the frequency axis. With the use of excitation of [7], the looped algorithms produce unperturbed distribution of electromagnetic fields for any mode in a periodic structure, at any frequency.

The spatially looped time-domain algorithms can be expressed in either complex or real notation. The real version requires 50% less computer resources. However, in application to periodic structures, the complex version is numerically more robust; operating the real version requires some expertise on the user's side. In application to single-layer models of uniform guiding structures, the real FDTD and TLM versions fully equivalent to the complex ones exist.

We have reached a number of original conclusions which concern the excitation of standing and traveling waves in the looped algorithms, and phase relationships between field components on the real and imaginary grid. These illustrate why the complex notation in the time domain cannot directly incorporate complex media parameters, and how it facilitates the numerical energy conservation. We hope that the reader will find our study helpful in understanding the consequences of the combined time-domain/phase shift-domain representation of electromagnetic fields.

References

[1] H. Jin, R. Vahldieck, and S. Xiao, "A full-wave analysis of arbitrary guiding structures using a two-dimensional TLM mesh," in *Proc. 21st Euro. Microwave Conf.*, Stuttgart, 1991, pp. 205–210.

[2] ——, "Full-wave analysis of guiding structures using a 2-D array of 3-D TLM nodes," *IEEE Trans. Microwave Theory Tech.*, vol. 41, pp. 472–477, Mar. 1993.

[3] F. Arndt, V. J. Brankovic, and D. V. Krupezevic, "An improved FD-TD full wave analysis for arbitrary guiding structures using a two-dimensional mesh," in *IEEE MTT Symp. Dig.,* Albuquerque, NM, 1992.
[4] S. Xiao, R. Vahldieck, and H. Jin, "Full-wave analysis of guided wave structures using a novel 2-D FD-TD," *IEEE Microwave and Guided Wave Lett.,* vol. 2, pp. 165–167, May 1992.
[5] C. Mroczkowski and W. K. Gwarek, "Microwave circuits described by two-dimensional vector wave equation and their analysis by FD-TD method," in *Proc. 21st Euro. Microwave Conf.,* Stuttgart, 1991, pp. 199–204.
[6] W. K. Gwarek, T. Morawski, and C. Mroczkowski, "Application of the FD-TD method to the analysis of circuits described by the two-dimensional vector wave equation," *IEEE Trans. Microwave Theory Tech.,* vol. 41, pp. 311–317, Feb. 1993.
[7] W. K. Gwarek and M. Celuch-Marcysiak, "Time-domain analysis of dispersive transmission lines," *Physique III,* pp. 581–591, Mar. 1993.
[8] M. Celuch-Marcysiak and W. K. Gwarek, "A transformed symmetrical condensed node for the effective TLM analysis of guided wave problems," *IEEE Trans. Microwave Theory Tech.,* vol. 41, pp. 820–823, May 1993.
[9] H. Guo *et al.,* "A novel highly accurate synthetic technique for determination of the dispersive characteristics in periodic slow wave circuits," *IEEE Trans. Microwave Theory Tech.,* vol. 40, pp. 2086–2094, Nov. 1992.
[10] P.-S. Kildal, "Artificially soft and hard surfaces in electromagnetics and their application to antenna design," in *Proc. 23rd Euro. Microwave Conf.,* Madrid, 1993, pp. 30–33.
[11] J. Esteban and J. M. Rebollar, "Characterization of corrugated waveguides by modal analysis," *IEEE Trans. Microwave Theory Tech.,* vol. 39, pp. 937–943, June 1991.
[12] W. K. Gwarek, "Analysis of arbitrarily-shaped planar circuit—A time-domain approach," *IEEE Trans. Microwave Theory Tech.,* vol. MTT-33, pp. 1067–1071, Oct. 1985.
[13] R. E. Collin, *Field Theory of Guided Waves.* New York: McGraw-Hill, 1960, ch. 9.1.
[14] M. Celuch-Marcysiak and W. K. Gwarek, "Effective time domain analysis of periodic structres," in *Proc. 23rd Euro. Microwave Conf.,* Madrid, 1993, pp. 293–295.

Malgorzata Celuch-Marcysiak was born in Warsaw, Poland, in 1964. She is a graduate of the United World Colleges. She received the M.Sc. degree (honors) in electronic engineering from the Warsaw University of Technology in 1988.

Currently she is working toward the Ph.D. degree at the Institute of Radioelectronics, Warsaw University of Technology. Her research interests are in the area of electromagnetic field theory and numerical analysis of microwave circuits, with emphasis on relationships between various numerical methods.

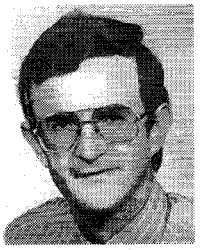

Wojciech K. Gwarek (SM'90) was born in Poland. He received the M.Sc. degree from Massachusetts Institute of Technology in 1974 and the Ph.D. and Habilitation degrees from the Warsaw University of Technology, Warsaw, Poland, in 1977 and 1988, respectively.

He is a professor at the Warsaw University of Technology. In 1992/1993 he participated in organizing the Franco-Polish School of New Information and Communication Technologies in Poznan. During the academic year 1991/1992 he was a visiting professor at Ecole Nationale Superieure de Tellecommunications de Bretagne, Brest, France. He is the author of many scientific papers, a textbook on electromagnetic theory, and a software package named QuickWave (distributed by ArguMens GmbH, Duisburg, Germany). His research interests are in the areas of electromagnetic field theory and computer-aided analysis and design of microwave circuits.

Dr. Gwarek is a Member of the Editorial Board of the IEEE TRANSACTIONS ON MICROWAVE THEORY AND TECHNIQUES and a Member of the Technical Programme Committee of the European Microwave Conference.